



OPEN ACCESS

EDITED BY

Vassil Traykov,

Acibadem City Clinic Tokuda Hospital, Bulgaria

REVIEWED BY

Florian Stöckigt,

Krankenhaus Porz am Rhein gGmbH,

Germany

Rahul Dhawan.

Pikeville Medical Center, United States

Hanxiona Liu

□ lhanx@126.com

Ashkan Ehdaie

ashkan.ehdaie@cshs.org

[†]These authors have contributed equally to this work and share first authorship

[‡]These authors have contributed equally to this work and share senior authorship

RECEIVED 30 June 2025 ACCEPTED 28 August 2025 PUBLISHED 16 September 2025

Yang G, Xiong S, Luo Y, Luo D, Shehata M, Zhang Z, Cai L, Wang X, Ehdaie A and Liu H (2025) The relative voltage index: a novel tailored method to identify left atrial low voltage areas in non-paroxysmal AF. Front. Cardiovasc. Med. 12:1656983. doi: 10.3389/fcvm.2025.1656983

COPYRIGHT

© 2025 Yang, Xiong, Luo, Luo, Shehata, Zhang, Cai, Wang, Ehdaie and Liu. This is an open-access article distributed under the terms of the Creative Commons Attribution License (CC BY). The use, distribution or reproduction in other forums is permitted, provided the original author(s) and the copyright owner(s) are credited and that the original publication in this journal is cited, in accordance with accepted academic practice. No use, distribution or reproduction is permitted which does not comply with

The relative voltage index: a novel tailored method to identify left atrial low voltage areas in non-paroxysmal AF

Guoshu Yang^{1†}, Shiqiang Xiong^{1†}, Yan Luo^{1†}, Duan Luo¹, Michael Shehata², Zhen Zhang¹, Lin Cai¹, Xunzhang Wang², Ashkan Ehdaie^{2*†} and Hanxiong Liu^{1*†}

¹Department of Cardiology, Affiliated Hospital of Southwest Jiaotong University, The Third People's Hospital of Chengdu, Chengdu, Sichuan, China, ²Smidt Heart Institute, Cedars Sinai Medical Center, Los Angeles, CA, United States

Background: The optimal voltage threshold for determining low voltage areas (LVA) in non-paroxysmal atrial fibrillation (NPAF) is unclear. This study aims to evaluate a patient-specific voltage measurement using the left atrial appendage (LAA) as a benchmark to establish a normalized threshold for detecting LVA in NPAF.

Methods: Bipolar LA and LAA voltage in 40 NPAF and 42 patients with no AF (control group) were studied in sinus rhythm (SR) and AF (NPAF group) and SR only in the control group. Bipolar LA and LAA voltage distribution were compared between the NPAF and control groups. Fibrotic regions identified by late gadolinium-enhanced magnetic resonance imaging (LGE-MRI) was used as the reference standard comparison in the NPAF group.

Results: The median, 5th percentile ($V_{LA5\%}$), and the 95th percentile of bipolar voltage in the LA were significantly lower in NPAF patients than controls. No significant LAA voltage differences between groups [median = 3.303 (1.796) vs. 3.100 (1.045); $V_{LAA95\%} = 8.089$ (3.571) vs. 7.604 (3.404), all p > 0.05]. A strong linear correlation between $V_{\text{LA5}\%}$ and $V_{\text{LAA95}\%}$ was observed in the control group. The standardized relative voltage index (RVI) factor of 0.1324 was identified as the threshold for defining LVA and calculated as $V_{LA5\%} = 0.1324 \times V_{LAA95\%}$. The correlation between LVA guided by RVI was superior to the universal threshold for detecting LVA in sinus and AF rhythms using LGE-MRI as the gold standard.

Conclusion: A patient-tailored low voltage threshold can be obtained using a simplified equation and provides more accurate representation of LVA in NPAF than universal thresholds

atrial fibrillation, electroanatomic mapping, fibrosis, low voltage areas, left atrium, left atrial appendage, magnetic resonance imaging

Introduction

Atrial fibrillation (AF), the most common cardiac arrhythmia, significantly contributes to increased risks of stroke, heart failure, and mortality (1, 2). Fibrosis of the left atrium (LA) represents a well-established pathological substrate that promotes both initiation and maintenance of AF (3). Notably, non-paroxysmal AF (NPAF) demonstrates greater fibrotic burden compared to paroxysmal AF (PAF) (4). This structural remodeling can

be non-invasively characterized through late gadolinium-enhanced magnetic resonance imaging (LGE-MRI), while electroanatomic mapping reveals corresponding low-voltage areas (LVA) (5–7). Substantial evidence confirms a robust correlation between LVA and atrial fibrosis in AF (8–12). Furthermore, the presence of LVA has been demonstrated as a significant predictor of AF recurrence following catheter ablation (13).

Although adjunctive LVA ablation has been proposed for NPAF substrate modification, clinical outcomes remain inconsistent (14). This variability may stem from non-standardized, patient-nonspecific LVA definitions. Thus, determining optimal voltage thresholds for clinically relevant LVA ablation targets in NPAF remains an area of ongoing research and debate. To address this knowledge gap, the aim of this study was to evaluate the feasibility of utilizing patient-specific voltage measurements from the left atrial appendage (LAA) as an intrinsic reference to establish a normalized LVA detection threshold in NPAF.

Materials & methods

Study population

A total of 82 patients were enrolled in the study between April 2017 and August 2022. The NPAF group included 40 patients (24 with persistent AF and 16 with long-standing persistent AF) who underwent initial radiofrequency catheter ablation (RFCA). The control group consisted of 42 patients with structurally normal hearts and no previous history of AF who underwent left-sided catheter ablation procedures [N=35] left-sided accessory pathway, N = 7 idiopathic ventricular premature contractions (VPC)]. NPAF was defined as AF episodes lasting ≥7 days. If sinus rhythm (SR) could not be restored by cardioversion prior to electroanatomic mapping, those NPAF patients were excluded from the study. All antiarrhythmic medications discontinued for a minimum of 5 half-lives, and amiodarone was ceased for a duration of 2 months prior to catheter ablation. Patient demographics, clinical characteristics, and medications details were obtained from electronic medical records.

This study was approved by the ethics committee of the Third People's Hospital of Chengdu and conducted in compliance with the ethical principles of the Declaration of Helsinki. All patients provided written informed consent.

The LGE-MRI study

The aim of the LGE-MRI study was to quantify the extent of fibrosis in the LA and LAA. Patients with NPAF underwent LGE-MRI of the LA and LAA using a 3-Tesla scanner (Siemens Skyra, Germany) and a 32-channel cardiac coil within 1 week before the

Abbreviations

NPFA, non-paroxysmal atrial fibrillation; SR, sinus rhythm; LVA, low voltage areas; LA, left atrium; LAA, left atrial appendage; RVI, relative voltage index; LGE-MRI, late gadolinium-enhanced magnetic resonance imaging.

electrophysiological assessment and/or ablation procedure. All patients were in atrial fibrillation (AF) during scanning.

The specific scanning protocol employed a 3D inversion recovery gradient-echo sequence, combined with respiratory navigation and electrocardiogram gating, and was performed 20 min after intravenous administration of gadolinium contrast agent (Gadobutrol, 0.2 mmol/kg). Scanning parameters were as follows: field of view, 350–390 mm; echo time (TE), 1.3–1.6 ms; repetition time (TR), 700–870 ms; inversion time, 310–350 ms; in-plane resolution, 1.37×1.37 mm; slice thickness, 1.5 mm; and voxel size, $1.25 \times 1.25 \times 2.5$ mm (reconstructed dimensions: $0.625 \times 0.625 \times 1.25$ mm). Additional typical acquisition parameters included: TR/TE, 5.5/3.0 ms; flip angle, 25° ; in-plane resolution, 1.25×1.25 mm; and slice thickness, 2.5 mm (reconstructed dimensions: $0.625 \times 0.625 \times 1.25$ mm).

For image post-processing, LGE CMR images were analyzed and segmented using MASS imaging software (Medis Medical Imaging Systems, Leiden, Netherlands). First, raw LGE CMR data were imported into the MASS software. The endocardial and epicardial contours of the LA were then manually delineated on each of the 96 cardiac MRI slices. Based on these segmentation results, the software automatically generated a 3D model of the LA. Myocardial tissue was classified by signal intensity ratio (SIR) as follows (15): healthy atrial myocardium (SIR < 1.2), interstitial fibrosis (SIR: 1.2–1.32), and dense scarring (SIR > 1.32).

Electrophysiology mapping and ablation procedure

In patients with NPAF, pre-procedure computerized tomography angiography images of the LA were obtained, and transesophageal echocardiography was performed within 48 h prior to the study to rule out left atrial thrombus. Catheter ablation procedures were performed under general anesthesia and muscular paralysis with hemodynamic and electrocardiographic monitoring. A decapolar coronary sinus catheter (2-5-2 mm interelectrode spacing, P-curve, Biosense Webster) was positioned via femoral venous approach under fluoroscopic guidance. Intravenous heparin was administered to maintain an activated clotting time of 300-350 s. Subsequently, LA access was obtained by transseptal puncture, through which a 20-polar mapping catheter (2 mm center-to-center spacing, Pentaray, Biosense Webster) was advanced to create the electroanatomic map. After mapping, a 3.5 mm tip irrigated ablation catheter (1-6-2 mm interelectrode spacing, ThermoCool SmartTouch, Biosense Webster) was advanced to perform ablation in the NPAF study group.

Intracardiac electrograms (EGMs) were recorded using an electrophysiological recording system (WorkMate Claris System, One St. Jude Medical, St. Paul, MN, USA) coupled with a three-dimensional electrophysiological navigating system (CARTO 3 system, Biosense Webster, Diamond Bar, CA, USA). EGM recording was filtered at 30–500 Hz. A detailed fast anatomic map (FAM) was performed with a distribution of points using a fill threshold of 15 mm and an internal point filter was set to limit electric potential data acquisition to within 5 mm from the

geometrical surface. The respiration gating method, which ensured the acquisition of anatomic points limited to the end period of expiration during mechanical ventilation, was adopted to minimize the breath related mapping shifts. The CONFIDENSE module (Biosense Webster) was used for tissue proximity detection and to assess adequate tissue-catheter contact of each acquired point during FAM. All mappings were performed by a single, highly experienced electrophysiologist, who implemented rigorous quality control both during real-time data acquisition and offline post-processing.

The following steps were performed to assess bipolar voltage in AF and SR in the NPAF group:

- 1. In patients presenting in AF, cardioversion was performed to obtain the first electroanatomic map in SR.
- AF was induced using atrial burst stimuli from the distal or midcoronary sinus at a cycle of 250–180 ms. Following a 5 min waiting period for rhythm stabilization, voltage mapping was conducted to create an electroanatomic map in AF.
- 3. Geometries of LA and LAA were created separately using Pentaray high density mapping catheter.
- 4. The LA geometrical surface was subdivided into 6 anatomical regions: anterior, posterior, roof, inferior, lateral, and septal (16).
- 5. Points within pulmonary veins (PVs) were excluded from the final analysis.

In consideration of temporal EGM amplitude variability during acquisition, each point was selected by recording a maximal peak-to-peak bipolar voltage amplitude value of local atrial EGM within window of interest during 10 consecutive QRS complexes (except atrial EGMs during each QRS duration). EGMs during premature beats were excluded. A goal of voltage mapping density was set to >200 points in LAA region and >500 points in LA.

In the control group, ablation of accessory pathway or VPC was performed after electroanatomic mapping of the LA and LAA in SR using the same technique as above for NPAF in SR.

Definitions

The bipolar voltage of dense scar was defined using the cut off value of 0.1 mV. Conventionally, any point with a bipolar voltage \leq 0.5 mV during SR was classified as a low voltage point. LVA were defined as sites of \geq 3 adjacent low voltage points, which were <5 mm apart. For the individualized LVA definition: sites with bipolar voltage \leq the normalized LVA detection threshold were designated as abnormal substrate. The borders of LVAs were automatically reconstructed in 3D using the CARTO® VOLTAGE VISITAGTM module.

Statistical analysis

Categorical data were presented as counts and percentages (%) and the comparison between two groups was assessed using the appropriate chi-square test. Continuous data were depicted as either the mean with standard deviation or the median with interquartile range (IQR), and the comparison between two groups was evaluated

using the *t*-test or Mann–Whitney *U*-test, respectively. Linear regression analysis was used to evaluate the relationships in LA and LAA voltages. The relationships between LA and LAA voltages with SR and AF were assessed using Spearman correlation coefficients. A two-tailed *p*-value less than 0.05 was considered statistically significant. All statistical analyses were performed with either SPSS statistics version 26.0 (IBM Corporation, Chicago, IL, USA) or GraphPad Prism software version 9.0 (GraphPad Software, CA, USA).

Results

Baseline characteristics

The baseline characteristics of all study participants are presented in Table 1. Compared to patients without AF, those with NPAF had larger LA, were older, male, and exhibited a higher prevalence of hypertension and coronary heart disease.

Electroanatomic mapping and bipolar voltage map

During SR, a mean of 422 ± 185 and 498 ± 372 bipolar voltage points per patient were analyzed in the LA for the control and NPAF group, respectively; An average of 276 ± 139 and 167 ± 67 bipolar voltage points per patient were analyzed in the LAA for the two groups, respectively.

Compared to patients without NPAF, the 5th, 25th, 50th, 75th, and 95th percentiles of bipolar voltage in the LA were significantly lower in patients with NPAF (Figure 1A). The bipolar voltage in the LAA was significantly higher than the LA in patients with NPAF, but not in the control group (Figure 1A). The median bipolar voltage in the LA was significantly lower in patients with NPAF when compared to the control group [2.970 (1.599) vs. 0.870 (0.560), P < 0.001; Figure 1B]. However, there was no significant difference in LAA bipolar voltage between the two groups [3.303 (1.796) vs. 3.100 (1.045), P > 0.05; Figure 1B]. The 5th and 95th percentiles of bipolar voltage in the LA were significantly lower in patients with NPAF compared to the control group [1.103 (0.529) vs. 0.085 (0.096), P < 0.001, Figure 1C; 7.937 (3.282) vs. 3.232 (2.087), P < 0.001, Figure 1D]. No significant difference was observed in the 95th percentile of bipolar voltage in the LAA (V_{LAA95%}) between the two groups [8.089 (3.571) vs. 7.604 (3.404), P > 0.05; Figure 1D]. The V_{LAA95%} in patients without NPAF conformed to a normal distribution. We used the $V_{LAA95\%}$ as a benchmark given the relative similarity in patients with and without AF.

Defining patient-specific normalized low voltage threshold

In previous studies, in control patients without AF, the 5th percentile of all LA mapping points ($V_{LA5\%}$) was designated as a bipolar voltage threshold indicating abnormal atrial substrate (17,

TABLE 1 Baseline characteristics.

| Variables | Control | NPAF (<i>n</i> = 40) | | | P value [*] | P value** |
|--|-------------------|-----------------------|--------------------|-----------------------------|----------------------|-----------|
| | | Total | Persistent AF | Long-standing persistent AF | | |
| | (n = 42) | | (n = 24) | (n = 16) | | |
| Age, years | 54.10 ± 16.48 | 64.15 ± 10.50 | 64.42 ± 11.67 | 63.75 ± 8.80 | 0.001 | 0.194 |
| Sex, male, <i>n</i> (%) | 19 (45.2) | 28 (70.0) | 17 | 11 | 0.023 | 0.888 |
| BMI | 23.11 ± 3.06 | 25.13 ± 3.60 | 25.12 ± 4.02 | 25.13 ± 2.96 | 0.008 | 0.277 |
| Smoking, n (%) | 11 (26.2) | 15 (37.5) | 11 (45.8) | 4 (25) | 0.271 | 0.182 |
| Congestive heart failure, n (%) | 1 (2.4) | 4 (10.0) | 2 (8.3) | 2 (12.5) | 0.15 | 0.667 |
| Hypertension, n (%) | 7 (16.7) | 21 (52.5) | 11 (45.8) | 10 (62.5) | 0.001 | 0.301 |
| Diabetes mellitus, n (%) | 6 (14.3) | 4 (10.0) | 4 (16.7) | 0 | 0.553 | 0.085 |
| Coronary heart disease, n (%) | 1 (2.4) | 12 (30.0) | 8 (33.3) | 4 (25) | 0.001 | 0.573 |
| Dyslipidemia, n (%) | 6 (14.3) | 4 (10.0) | 3 (12.5) | 1 (6.25) | 0.553 | 0.519 |
| Obstructive sleep apnea, n (%) | 0 (0) | 2 (5.0) | 2 (8.3) | 0 | 0.142 | 0.236 |
| Prior stroke, n (%) | 1 (2.4) | 4 (10.0) | 3 (12.5) | 1 (6.25) | 0.150 | 0.519 |
| CHA ₂ DS ₂ -VASC score | - | 2.42 ± 1.30 | 2.42 ± 1.21 | 2.44 ± 1.46 | - | 0.229 |
| BNP (pg/ml) | 96.5 (35, 121.98) | 94.6 (49.6, 341.1) | 154.75 (67, 98.03) | 164.55 (97.63, 320.08) | 0.049 | 0.023 |
| eGFR (ml/min*1.73 m ²) | 98.11 ± 20.36 | 90.98 ± 20.22 | 92.19 ± 19.14 | 89.16 ± 22.27 | 0.116 | 0.771 |
| LAD (mm) | 35.43 ± 4.62 | 42.95 ± 5.25 | 42.13 ± 5.21 | 44.19 ± 5.23 | 0.000 | 0.705 |
| LVDd (mm) | 45 (41.75, 48) | 47 (44, 50) | 47 (43, 50) | 47 (44.25, 50) | 0.166 | 0.793 |
| LVEF (%) | 60 (58, 63.25) | 58.5 (57, 62) | 58.5 (56.25, 62) | 58.5 (57, 61.75) | 0.000 | 0.883 |
| Time since AF onset, day | - | 365 (30, 1,095) | 60 (10, 333.75) | 1,642.5 (730, 3,011.25) | - | <0.001 |

The baseline characteristics of the individuals with or without NPAF.

NPAF, non-paroxysmal atrial fibrillation; BMI, body mass index; BNP, brain natriuretic peptide; eGFR, estimated glomerular filtration rate; LAD, left atrial diameter; LVDd, left ventricular diastolic dimension; LVEF, left ventricular ejection fraction.

18). Thus, a point with a voltage lower than $V_{LA5\%}$ was defined as low voltage. In the present study, a strong linear correlation between $V_{LA5\%}$ and $V_{LAA95\%}$ (P < 0.0001, $V_{LA5\%} = 0.1324 \times V_{LAA95\%}$, Figure 2A) was observed in the control group. The ratio of each point's voltage to $V_{LAA95\%}$ in each patient was termed the *relative voltage index* (RVI). When adjusting each point's voltage in the LAA and LA by $V_{LAaA95\%}$ and expressing them as RVI, the scattergrams revealed a notably stronger linear correlation of the electrogram amplitudes between SR and AF (Figures 2B,D). However, when directly using the absolute voltage of each point (AVI) in the LAA and LA, the scattergrams displayed a significant but weaker linear correlation of the bipolar voltage between SR and AF (Figures 2C,E).

Paired t-tests revealed that the absolute voltage index (AVI) values of the LA and LAA exhibited statistically significant differences in the same patient between SR and atrial AF states. In contrast, the RVI showed no statistically significant differences between SR and AF states in either the LA or LAA regions (Figures 3A,B). These results suggest that the correlation between $V_{\rm LAA95\%}$ and $V_{\rm LA5\%}$ established in control patients could applicability to patients with NPAF. These results suggest that the correlation between $V_{\rm LAA95\%}$ and $V_{\rm LA5\%}$ established in control patients could be applicable to patients with NPAF.

Determination of V_{LA5%} in NPAF patients

In the control group, the RVI of $V_{LA5\%}$ to $V_{LAA95\%}$ approaches a constant as indicated by the regression equation mentioned above. This constant was identified as the standard relative voltage index (SRVI) in this study, serving as the threshold value for the RVI

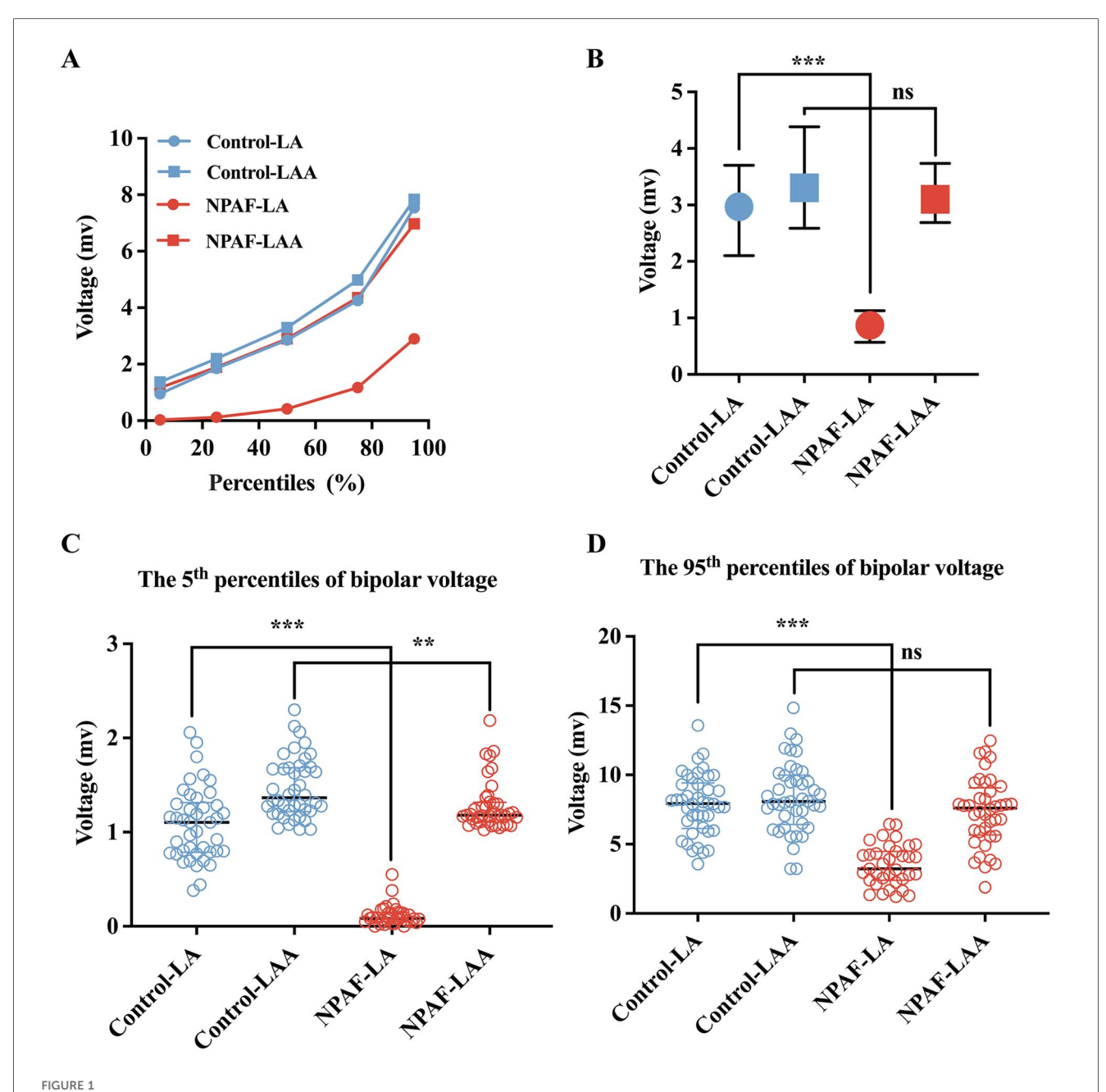
criterion in defining LVA. The $V_{\rm LA5\%}$ of normal LA is defined as the low voltage threshold value, and any point with a voltage lower than "normal" $V_{\rm LA5\%}$ should be classified as a low voltage point for that patient. However, the "normal" $V_{\rm LA5\%}$ in a patient with NPAF is unavailable due to diseased myocardium. Herein, the "normal" $V_{\rm LA5\%}$ for each NPAF patient can be calculated with the equation: $V_{\rm LA5\%}=0.1324\times V_{\rm LA495\%}.$

LVA determined by different threshold settings to match LGE-MRI

Following electroanatomic mapping of the LA and LAA, V_{LAA95%} is determined. Utilizing $V_{LA5\%} = 0.1324 \times V_{LAA95\%}$, the patient-specific $V_{LA5\%}$ is calculated, which functions as the normalized threshold for identifying LVA within the LA in patients with NPAF. In the cohort of 40 NPAF patients, the SRVI-guided substrate mapping can be visually appreciated as a better match to the fibrotic regions of LGE in both rhythms as compared to the conventional voltage threshold for LVA (Table 2). Two retrospective cases of NPAF were presented to compare the distributions of LVA defined by SRVI and conventional threshold of 0.5 mV with fibrosis regions of LGE-MRI in both AF and SR (Figure 4). The V_{LA5%} for Case 1 was 0.85 mV in AF and 1.0 mV in SR (Figures 4A,B). For Case 2, the V_{LA5%} was 0.28 mV in AF and 0.32 mV in SR (Figures 4C,D). In comparison to the conventional LVA threshold of 0.5 mV, LVA in both the anterior and posterior walls of the LA in NPAF

^{*}P value, Control vs. NPAF.

^{**}P value, Persistent AF vs. Long-standing AF.

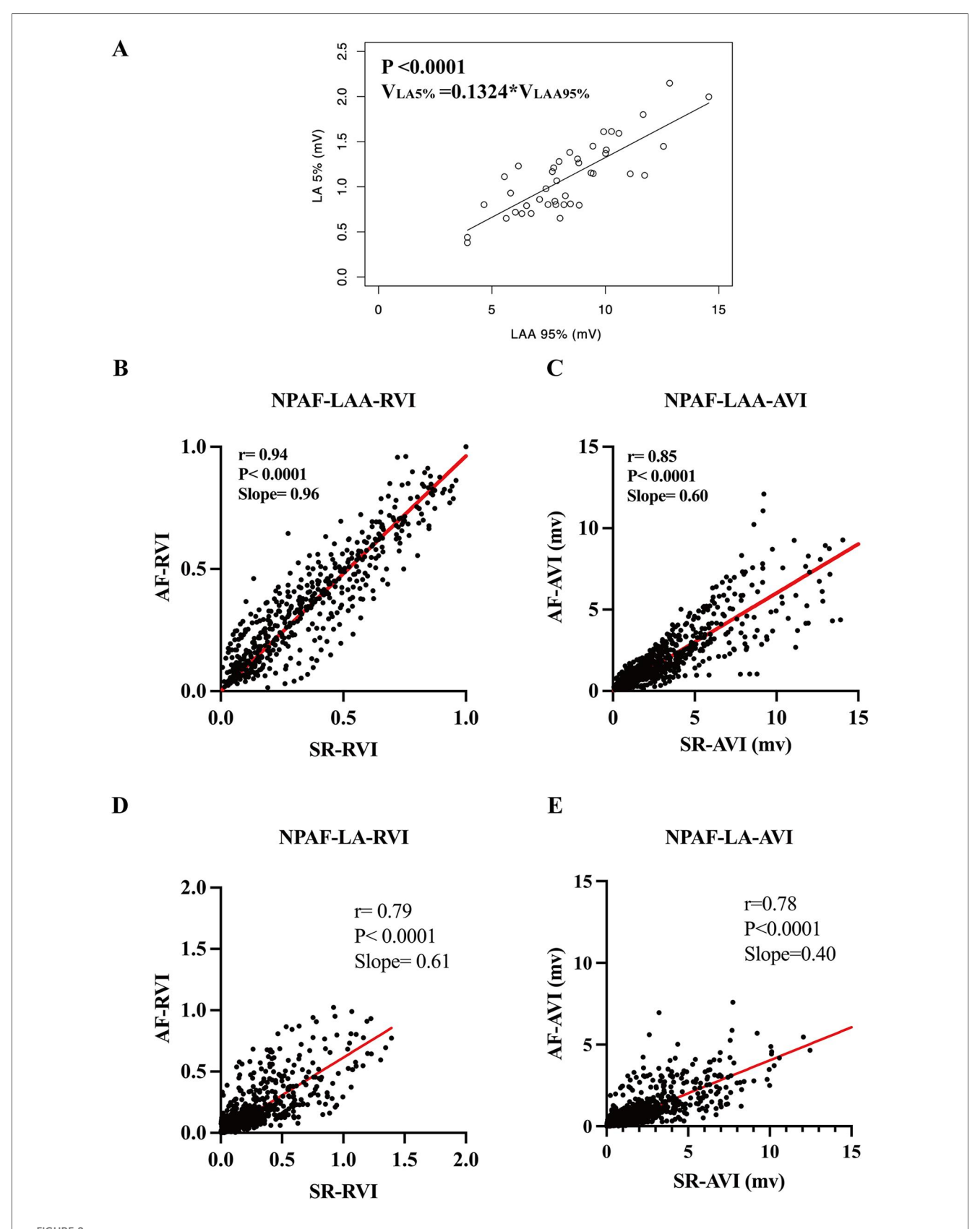


Bipolar voltage comparisons between the LA and LAA. (A) The 5th, 25th, 50th, 75th, and 95th percentiles of the bipolar voltage for the LA and LAA in the Control group and NPAF group obtained during SR. (B) Voltage for the LA and LAA in the Control group and NPAF group. (C) The 5th percentile of voltage in the LA and LAA during SR. (D) The 95th percentile of voltage in the LA and LAA during SR. NPAF, non-paroxysmal atrial fibrillation; LA, left atrium; LAA, left atrial appendage; SR, sinus rhythm. ***, P < 0.001; **, P < 0.01; ns, no significance. Data are expressed as the median and interquartile range.

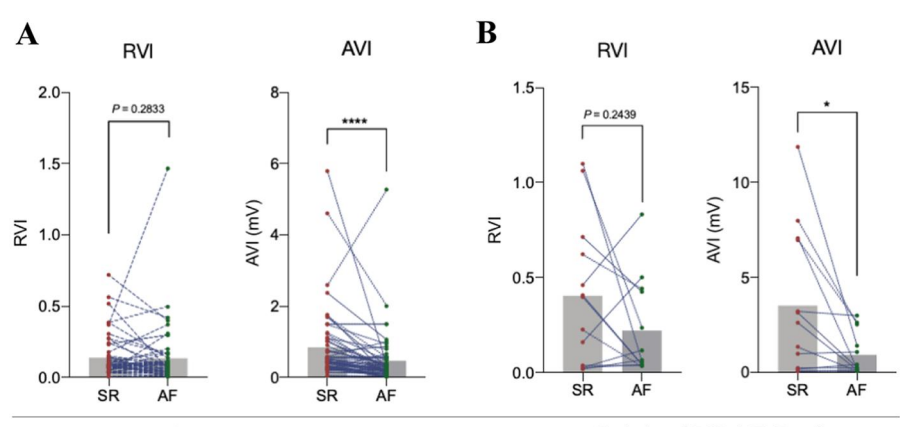
patients during AF, as defined by the normalized criteria-guided substrate mapping, exhibited a stronger correlation with the fibrotic regions of LGE.

The distribution and extent of LVA determined by different threshold settings

A low voltage index was employed to define the heterogeneity of the bipolar voltage amplitude by computing the coefficient of variance (standard deviation/mean value) of the voltage of all points (18). The regional and overall differences in the low voltage index based on SRVI and conventional LVA detection threshold of 0.5 mV in both rhythms are summarized in Table 3. During both rhythms, the low voltage index was significantly higher in AF than SR across all LA segments, regardless of the threshold settings. The correlation between the low voltage index in both rhythms, as defined by the normalized RVI-guided substrate mapping, was superior to the conventional LVA detection threshold value of 0.5 mV.



Establishment and validation of a normalized relative voltage index equation. (A) The regression equation of the 5th percentile of voltage in the LA $(V_{LA 95\%})$ and the 95th percentile of voltage in the LAA $(V_{LA 95\%})$ used in the normalized RVI threshold equation. Note correlation of the RVI in the LAA (B) and the LA (D) in SR and AF rhythm. Comparisons made to the AVI in the LAA and LA in SR and AF rhythm are shown in (C,E), respectively. RVI, relative voltage index; AVI, absolute voltage index. Other abbreviations as per Figure 1.



LA of NPAF Patients

LAA of NPAF Patients

FIGURE 3

Establishing the applicability of the relative voltage index to patients with Non-paroxysmal atrial fibrillation. (A) Pairwise t-test of mapping results in LA for sinus rhythm (SR) and atrial fibrillation (AF) under relative voltage index (RVI) and absolute voltage index (AVI) in patients with non-paroxysmal atrial fibrillation (NPAF), n = 40. (B) Pairwise t-test of mapping results in LAA for SR and AF under RVI and AVI in patients with NPAF, n = 40.

TABLE 2 Comparing the efficacy of SRVI and AVI in detecting left atrial LVA in NPAF.

| Imaging view | SRVI (n = 40) | Conventional setting (0.5 mV) | P value |
|----------------|------------------|-------------------------------|---------|
| AP view, n (%) | 26 (65) | 15 (37.5) | 0.014 |
| PA view, n (%) | 23 (57.5) | 13 (32.5) | 0.025 |

Visual comparison of the performance of the SRVI and the conventional voltage threshold (<0.5 mV) in detecting LVA based on MRI-defined fibrosis. SRVI, standard relative voltage index; LVA, low voltage areas. AP (anterior to posterior) and PA (posterior to anterior) views reference the imaging angle used to visualize the left atrium.

Discussion

To the best of our knowledge, this study is the first to evaluate a novel patient-specific definition of LVA using a simplified equation in NPAF.

The main findings are as follows:

- A novel patient-specific SRVI threshold for low voltage outperforms conventional voltage thresholds for LVA and can be used in SR or AF.
- Unlike LA voltage, LAA bipolar voltage amplitudes are not significantly different between patients with normal LA and patients with NPAF.
- 3. There is a strong linear correlation between $V_{\rm LA5\%}$ and $V_{\rm LAA95\%}$ in the normal LA.

Significance of voltage differences by electroanatomic mapping

The origin of low amplitude atrial electrograms can be multifactorial but atrial fibrosis is considered a primary structural cause (19). Bipolar voltage mapping is used as a surrogate for identification of histopathological LA fibrosis

despite inherent limitations (8–10, 13, 20). Studies have demonstrated a strong correlation between bipolar voltage mapping and LGE-MRI, which is considered the gold standard for identification of LA fibrosis (5, 6). However, there is no unified criteria for detecting LVA in patients with NPAF across different rhythms and with different recording electrodes. Voltage is influenced by the extent of LA fibrosis which relates to clinical factors such as age, LA size, comorbidities, and duration of AF (18, 21, 22). Voltage is also affected by the rhythm mapped, regional wall thickness, and the duration of acquisition (21–25). Using a universal absolute voltage cut-off to define LVA in NPAF disregards the variable factors that may influence bipolar voltage in each individual case. Our study refines the definition of LVA in NPAF to account for a population with heterogeneous fibrotic burden and distribution.

Validation of voltage thresholds for defining LVA

Voltage thresholds to identify low voltage have been classified based on the 95th percentile of voltage in patients with and without AF (17, 18, 26). Multiple thresholds have been reported for identifying LVA across different phenotypes of AF (PAF and NPAF) during both AF and SR. A universal constant, such as 0.5 mV and 0.4 mV, has been established as the absolute threshold for identifying LVA in AF patients (18, 27–29). Fibrotic burden by MRI remains the gold standard for identification of substrate. Low voltage thresholds have limited specificity and sensitivity for detection of fibrosis by MRI but appear to be more predictive when mapping in AF as compared to SR (25). Using the LAA voltage as a reference, the equation for determining a normalized LVA threshold value in the LA for NPAF is highlighted in the current study $(V_{LA5\%} = 0.1324 \times V_{LAA95\%})$. We have validated this voltage

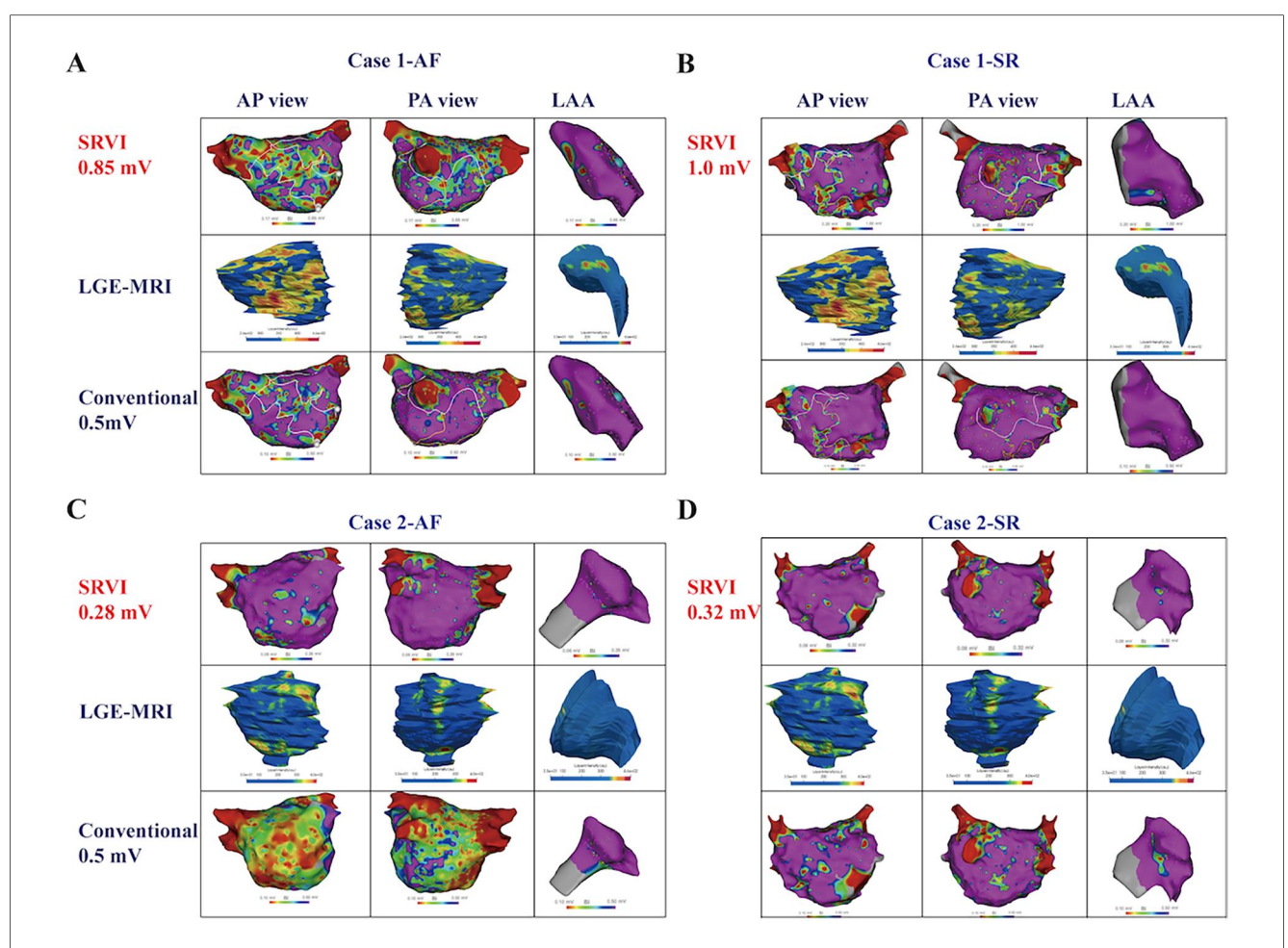


FIGURE 4

Comparison between SRVI defined LVA and conventional voltage threshold in NPAF patients. Case 1. Comparison between LVA defined by SRVI [<0.85 mV in AF (A) and <1.0 mV in SR (B)] and the conventional low voltage threshold of <0.5 mV and correlation with LGE on cardiac MRI. Note the visual underestimation of fibrosis in the conventional voltage threshold as compared to LGE especially in AF whereas the SRVI provides a more accurate representation. Case 2. Comparison between LVA defined by SRVI [<0.28 mV in AF (C) and <0.32 mV in SR (D)] and the conventional low voltage threshold of <0.5 mV and correlation with LGE on cardiac MRI. Note the visual overestimation of fibrosis based on conventional voltage thresholds especially in AF whereas the SRVI provides a more accurate representation. LGE-MRI, late gadolinium enhancement MRI; SRVI, standard relative voltage index. Other abbreviations as per Figure 1.

TABLE 3 The extent of LVA detected by different threshold settings.

| Anatomical region | SRVI | | Conventional setting (0.5 mV) | | |
|-------------------|----------------|----------------|-------------------------------|----------------|--|
| | SR (n = 40) | AF (n = 40) | SR (n = 40) | AF (n = 40) | |
| LAA (%) | 26.09 ± 12.95 | 23.91 ± 15.44 | 15.44 ± 12.27 | 20.06 ± 15.33 | |
| Anterior (%) | 62.39 ± 19.03 | 71.84 ± 25.20 | 37.92 ± 23.32 | 63.04 ± 27.39 | |
| Inferior (%) | 50.05 ± 21.10 | 73.10 ± 19.83 | 29.41 ± 18.87 | 61.95 ± 23.60 | |
| Septal (%) | 65.36 ± 18.17 | 71.92 ± 22.14 | 41.07 ± 19.23 | 64.21 ± 24.11 | |
| Lateral (%) | 40.63 ± 24.49 | 63.77 ± 23.72 | 31.44 ± 24.23 | 56.21 ± 26.15 | |
| Posterior (%) | 53.55 ± 23.51 | 68.35 ± 21.45 | 34.28 ± 25.14 | 59.14 ± 25.92 | |
| Roof (%) | 53.51 ± 27.83 | 75.07 ± 24.82 | 35.07 ± 28.54 | 63.03 ± 31.46 | |
| LA (%) | 54.11 ± 18.70 | 70.33 ± 17.34 | 34.74 ± 19.50 | 61.10 ± 23.37 | |

LVA, low voltage areas; SR, sinus rhythm; AF, atrial fibrillation; SRVI, standard relative voltage index; LAA, left atrial appendage; LA, left atrium.

index with gold standard MRI in our study and provided a more accurate representation of histopathological fibrosis during electroanatomic mapping.

Use of the LAA in normalizing bipolar voltage

The observed voltage discrepancy between the LAA as compared to the LA in NPAF is consistent with the study by Yagishita et al. noting that the highest voltages were observed in the LAA in patients with PAF and NPAF in SR and AF (24). Our study expands the analysis to patients with normal LA (control group—no PAF or NPAF). We found no significant difference in the distribution of LAA voltage between the control group and NPAF group during SR, especially for the V_{LAA95%}. Notably, we extended this observation by including a control cohort (patients with normal LA, no PAF/NPAF) and demonstrating selective preservation of LAA voltage in NPAF: while all LA voltage percentiles (5th, 25th, 50th, 75th, 95th) were significantly lower in NPAF vs. controls, LAA voltage—including V_{LAA95%}—has no significant difference between groups (median LAA voltage: 3.303 [1.796] vs. 3.100 [1.045],

P > 0.05; V_{LAA95%}: 8.089 [3.571] vs. 7.604 [3.404], P > 0.05) during SR. This stability indicates the electrophysiological characteristics of LAA is spared from the structural remodeling that drives LA voltage attenuation in NPAF.

Consistent with prior studies in NPAF, which have demonstrated a lower LGE burden in the LAA compared with the LA, this reduced fibrotic involvement may explain the LAA's electrophysiological stability (18, 25). Factors that may make the LAA less susceptible to fibrosis include a lower proportion of interstitial cells, robust arterial supply, and enhanced wall thickness (30, 31). Intuitively, the LAA voltage (V_{LAA95%}) would be the most appropriate benchmark to establish a standard RVI for detection of LVA in each case of NPAF.

Rhythm-dependent low voltage assessment

Studies exploring the relationship between bipolar voltage in SR and AF have had mixed results. Linear correlations have been shown but the influence of other electrophysiological factors such as electrogram fractionation may play a significant role in voltage differences between SR and AF (22, 24). Moisés et al. suggested that bipolar voltage thresholds for LVA should be adjusted depending on the rhythm and found that employing a modified lower detection threshold for LVA during mapping might produce valid and reliable results for identifying regions with a voltage of <0.5 mV in SR (23). There is a paucity of data on the ideal voltage threshold for identifying LVA in AF, however. Differences due to wavefront collision, spiral waves, and critical repolarization/depolarization mass may result in significant voltage threshold changes in SR vs. AF. In one study, the LVA threshold during AF was half of the standard threshold used in SR (23). Variability in AF cycle length, location of recording, and substrate heterogeneity may limit the reproducibility of LVA thresholds when used during AF. The personalized RVI that we have proposed in this study simplifies the assessment of LVA during electroanatomic mapping. Our findings suggest that the RVI can be used for LVA assessment in a rhythm-independent fashion.

Clinical implications

A simplified and tailored approach to LVA threshold assessment with the RVI enhances the identification of atrial substrate in each individual patient without the influence of the type of rhythm. This may lead to improved efficiency of mapping and a better understanding of the underlying pathology for prognostication, especially if advanced cardiac imaging (LGE-MRI) is unavailable or undesired. Whether the use of RVI can more accurately identify and improve outcomes after voltage-based extra-pulmonary vein substrate modification during AF catheter ablation is unknown and deserves further investigation.

Study limitations

There were several limitations in our study. Patients with AF at the beginning of the case were cardioverted to SR for the first mapping study. This may not be achievable in all cases of NPAF. Although our LA mapping density meets current high-density standards, we acknowledge it may be relatively low depending on the contemporary mapping system used; future studies employing ultra-high-density mapping could potentially achieve finer substrate characterization. Voltage measurements in SR may be underestimated due stunned myocardium after cardioversion. Apart from comparing bipolar voltage, we did not analyze other electrogram characteristics, such as unipolar voltage, cycle length, fractionated electrograms, and rotational activity across varied voltage settings and rhythms. We also did not explore the influence of additional wavefronts during sinus rhythm on voltage amplitudes. Additionally, prior studies have shown that patients with left-sided accessory pathways [which constitute the majority of Wolff-Parkinson-White (WPW) syndrome cases] exhibit a significantly higher prevalence of AF compared to the general population, with paroxysmal AF occurring in up to onethird of WPW patients (32, 33). This association indicates that left-sided accessory pathways are linked to an atrial substrate with heightened AF susceptibility and the selection of such patients as the control group may introduce potential confounding.

Conclusions

A patient-tailored, rhythm-independent, low voltage threshold index can be obtained using a simplified equation and provides a more accurate representation of LVA in NPAF than universal voltage thresholds.

Data availability statement

The original contributions presented in the study are included in the article/Supplementary Material, further inquiries can be directed to the corresponding authors.

Ethics statement

The studies involving humans were approved by the ethics committee of the Third People's Hospital of Chengdu. The studies were conducted in accordance with the local legislation and institutional requirements. The participants provided their written informed consent to participate in this study.

Author contributions

GY: Writing – original draft, Methodology. SX: Funding acquisition, Writing – original draft, Formal analysis. YL:

Formal analysis, Investigation, Data curation, Writing – review & editing. DL: Data curation, Writing – review & editing, Investigation. MS: Conceptualization, Writing – review & editing. ZZ: Conceptualization, Writing – review & editing. LC: Writing – review & editing, Conceptualization. XW: Conceptualization, Writing – review & editing. AE: Validation, Writing – review & editing. HL: Funding acquisition, Validation, Supervision, Writing – review & editing.

Funding

The author(s) declare that financial support was received for the research and/or publication of this article. This study was supported by the grant from Liu Hanxiong Famous Doctor Studio of Chengdu (20240216), the Natural Science Foundation of Sichuan Province (2024NSFSC1709), and the Scientific Research Project of The Third People's Hospital of Chengdu (CSY-YN-01-2023-041).

Conflict of interest

The authors declare that the research was conducted in the absence of any commercial or financial relationships that could be construed as a potential conflict of interest.

References

- 1. Stewart S, Hart CL, Hole DJ, McMurray JJ. A population-based study of the long-term risks associated with atrial fibrillation: 20-year follow-up of the renfrew/paisley study. *Am J Med.* (2002) 113:359–64. doi: 10.1016/S0002-9343(02)01236-6
- 2. Lloyd-Jones DM, Wang TJ, Leip EP, Larson MG, Levy D, Vasan RS, et al. Lifetime risk for development of atrial fibrillation: the framingham heart study. *Circulation*. (2004) 110:1042–6. doi: 10.1161/01.CIR.0000140263.20897.42
- 3. Dzeshka MS, Lip GY, Snezhitskiy V, Shantsila E. Cardiac fibrosis in patients with atrial fibrillation: mechanisms and clinical implications. *J Am Coll Cardiol.* (2015) 66:943–59. doi: 10.1016/j.jacc.2015.06.1313
- 4. Platonov PG, Mitrofanova LB, Orshanskaya V, Ho SY. Structural abnormalities in atrial walls are associated with presence and persistency of atrial fibrillation but not with age. *J Am Coll Cardiol.* (2011) 58:2225–32. doi: 10.1016/j.jacc.2011.05.061
- 5. Mahnkopf C, Badger TJ, Burgon NS, Daccarett M, Haslam TS, Badger CT, et al. Evaluation of the left atrial substrate in patients with lone atrial fibrillation using delayed-enhanced MRI: implications for disease progression and response to catheter ablation. *Heart Rhythm.* (2010) 7:1475–81. doi: 10.1016/j.hrthm.2010.06.030
- 6. Oakes RS, Badger TJ, Kholmovski EG, Akoum N, Burgon NS, Fish EN, et al. Detection and quantification of left atrial structural remodeling with delayed-enhancement magnetic resonance imaging in patients with atrial fibrillation. *Circulation*. (2009) 119:1758–67. doi: 10.1161/CIRCULATIONAHA.108.811877
- Bijvoet GP, Nies H, Holtackers RJ, Linz D, Adriaans BP, Nijveldt R, et al. Correlation between cardiac MRI and voltage mapping in evaluating atrial fibrosis: a systematic review. *Radiol Cardiothorac Imaging*. (2022) 4:e220061. doi: 10.1148/rvct.220061
- 8. Junarta J, Siddiqui MU, Riley JM, Dikdan SJ, Patel A, Frisch DR. Low-voltage area substrate modification for atrial fibrillation ablation: a systematic review and meta-analysis of clinical trials. *Europace*. (2022) 24:1585–98. doi: 10.1093/europace/euac089
- 9. Siebermair J, Kholmovski EG, Marrouche N. Assessment of left atrial fibrosis by late gadolinium enhancement magnetic resonance imaging: methodology and clinical implications. *JACC Clin Electrophysiol.* (2017) 3:791–802. doi: 10.1016/j.jacep.2017. 07 004
- 10. Liu W, Li S, Han B. It is necessary to re-understand the low-voltage area in atrial fibrillation patients. *Front Cardiovasc Med.* (2022) 9:919873. doi: 10.3389/fcvm.2022.919873

Generative AI statement

The author(s) declare that no Generative AI was used in the creation of this manuscript.

Any alternative text (alt text) provided alongside figures in this article has been generated by Frontiers with the support of artificial intelligence and reasonable efforts have been made to ensure accuracy, including review by the authors wherever possible. If you identify any issues, please contact us.

Publisher's note

All claims expressed in this article are solely those of the authors and do not necessarily represent those of their affiliated organizations, or those of the publisher, the editors and the reviewers. Any product that may be evaluated in this article, or claim that may be made by its manufacturer, is not guaranteed or endorsed by the publisher.

Supplementary material

The Supplementary Material for this article can be found online at: https://www.frontiersin.org/articles/10.3389/fcvm.2025. 1656983/full#supplementary-material

- 11. Yamaguchi T, Otsubo T, Takahashi Y, Nakashima K, Fukui A, Hirota K, et al. Atrial structural remodeling in patients with atrial fibrillation is a diffuse fibrotic process: evidence from high-density voltage mapping and atrial biopsy. *J Am Heart Assoc.* (2022) 11:e024521. doi: 10.1161/JAHA.121.024521
- 12. Caixal G, Alarcón F, Althoff TF, Nuñez-Garcia M, Benito EM, Borràs R, et al. Accuracy of left atrial fibrosis detection with cardiac magnetic resonance: correlation of late gadolinium enhancement with endocardial voltage and conduction velocity. *Europace*. (2021) 23:380–8. doi: 10.1093/europace/euaa313
- 13. Verma A, Wazni OM, Marrouche NF, Martin DO, Kilicaslan F, Minor S, et al. Pre-existent left atrial scarring in patients undergoing pulmonary vein antrum isolation: an independent predictor of procedural failure. *J Am Coll Cardiol.* (2005) 45:285–92. doi: 10.1016/j.jacc.2004.10.035
- 14. Moustafa A, Karim S, Kahaly O, Elzanaty A, Meenakshisundaram C, Abi-Saleh B, et al. Low voltage area guided substrate modification in nonparoxysmal atrial fibrillation: a systematic review and meta-analysis. *J Cardiovasc Electrophysiol.* (2023) 34:455–64. doi: 10.1111/jce.15764
- 15. Benito EM, Carlosena-Remirez A, Guasch E, Prat-González S, Perea RJ, Figueras R, et al. Left atrial fibrosis quantification by late gadolinium-enhanced magnetic resonance: a new method to standardize the thresholds for reproducibility. *Europace*. (2017) 19:1272–9. doi: 10.1093/europace/euw219
- 16. Huang W, Sun H, Xiong S, Luo Y, Tang Y, Zhang Z, et al. Sex-related differences in left atrial substrate among patients with atrial fibrillation: evidence from high-density voltage mapping. *Eur J Med Res.* (2024) 29:354. doi: 10.1186/s40001-024-01952-y
- 17. Saghy L, Callans DJ, Garcia F, Lin D, Marchlinski FE, Riley M, et al. Is there a relationship between complex fractionated atrial electrograms recorded during atrial fibrillation and sinus rhythm fractionation? *Heart Rhythm*. (2012) 9:181–8. doi: 10. 1016/j.hrthm.2011.09.062
- 18. Lin Y, Yang B, Garcia FC, Ju W, Zhang F, Chen H, et al. Comparison of left atrial electrophysiologic abnormalities during sinus rhythm in patients with different type of atrial fibrillation. *J Interv Card Electrophysiol.* (2014) 39:57–67. doi: 10.1007/s10840-013-9838-y
- 19. Allessie M, Ausma J, Schotten U. Electrical, contractile and structural remodeling during atrial fibrillation. *Cardiovasc Res.* (2002) 54:230–46. doi: 10. 1016/S0008-6363(02)00258-4

20. Marrouche NF, Wilber D, Hindricks G, Jais P, Akoum N, Marchlinski F, et al. Association of atrial tissue fibrosis identified by delayed enhancement MRI and atrial fibrillation catheter ablation: the DECAAF study. *Jama*. (2014) 311:498–506. doi: 10. 1001/jama.2014.3

- 21. Mannion J, Hong K, Lennon SJ, Kenny A, Galvin J, O'Brien J, et al. Comparing left atrial low voltage areas in sinus rhythm and atrial fibrillation using novel automated voltage analysis: a pilot study. *Cardiol Res.* (2023) 14:268–78. doi: 10.14740/cr1503
- 22. Masuda M, Fujita M, Iida O, Okamoto S, Ishihara T, Nanto K, et al. Comparison of left atrial voltage between sinus rhythm and atrial fibrillation in association with electrogram waveform. *Pacing Clin Electrophysiol*. (2017) 40:559–67. doi: 10.1111/pace.13051
- 23. Rodríguez-Mañero M, Valderrábano M, Baluja A, Kreidieh O, Martínez-Sande JL, García-Seara J, et al. Validating left atrial low voltage areas during atrial fibrillation and atrial flutter using multielectrode automated electroanatomic mapping. *JACC Clin Electrophysiol.* (2018) 4:1541–52. doi: 10.1016/j.jacep.2018.08.015
- 24. Yagishita A, De Oliveira S, Cakulev I, Gimbel JR, Sparano D, Manyam H, et al. Correlation of left atrial voltage distribution between Sinus rhythm and atrial fibrillation: identifying structural remodeling by 3-D electroanatomic mapping irrespective of the rhythm. *J Cardiovasc Electrophysiol.* (2016) 27:905–12. doi: 10. 1111/jce.13002
- 25. Qureshi NA, Kim SJ, Cantwell CD, Afonso VX, Bai W, Ali RL, et al. Voltage during atrial fibrillation is superior to voltage during sinus rhythm in localizing areas of delayed enhancement on magnetic resonance imaging: an assessment of the posterior left atrium in patients with persistent atrial fibrillation. *Heart Rhythm.* (2019) 16:1357-67. doi: 10.1016/j.hrthm.2019.05.032
- 26. Kapa S, Desjardins B, Callans DJ, Marchlinski FE, Dixit S. Contact electroanatomic mapping derived voltage criteria for characterizing left atrial scar

- in patients undergoing ablation for a trial fibrillation. J Cardiovasc Electrophysiol. (2014) 25:1044–52. doi: 10.1111/jce.12452
- 27. Yang G, Yang B, Wei Y, Zhang F, Ju W, Chen H, et al. Catheter ablation of nonparoxysmal atrial fibrillation using electrophysiologically guided substrate modification during Sinus rhythm after pulmonary vein isolation. *Circ Arrhythm Electrophysiol.* (2016) 9:e003382. doi: 10.1161/CIRCEP.115.003382
- 28. Yagishita A, Gimbel JR, De Oliveira S, Manyam H, Sparano DI, Cakulev IV, et al. Long-term outcome of left atrial voltage-guided substrate ablation during atrial fibrillation: a novel adjunctive ablation strategy. *J Cardiovasc Electrophysiol.* (2017) 28:147–55. doi: 10.1111/jce.13122
- 29. Lo LW, Tai CT, Lin YJ, Chang SL, Wongcharoen W, Chang SH, et al. Progressive remodeling of the atrial substrate-a novel finding from consecutive voltage mapping in patients with recurrence of atrial fibrillation after catheter ablation. *J Cardiovasc Electrophysiol.* (2007) 18:258–65. doi: 10.1111/j.1540-8167. 2007.00719.x
- 30. Naksuk N, Padmanabhan D, Yogeswaran V, Asirvatham SJ. Left atrial appendage: embryology, anatomy, physiology, arrhythmia and therapeutic intervention. *JACC Clin Electrophysiol.* (2016) 2:403–12. doi: 10.1016/j.jacep.2016.06.006
- 31. Spach MS, Dolber PC. Relating extracellular potentials and their derivatives to anisotropic propagation at a microscopic level in human cardiac muscle. Evidence for electrical uncoupling of side-to-side fiber connections with increasing age. *Circ Res.* (1986) 58:356–71. doi: 10.1161/01.RES.58.3.356
- 32. Sharma AD, Klein GJ, Guiraudon GM, Milstein S. Atrial fibrillation in patients with Wolff-Parkinson-White syndrome: incidence after surgical ablation of the accessory pathway. *Circulation*. (1985) 72:161–9. doi: 10.1161/01.CIR.72.1.161
- 33. Haissaguerre M, Fischer B, Labbé T, Lemétayer P, Montserrat P, d'Ivernois C, et al. Frequency of recurrent atrial fibrillation after catheter ablation of overt accessory pathways. *Am J Cardiol.* (1992) 69(5):493–7. doi: 10.1016/0002-9149(92)90992-8